Supporting Information for

Oxygen-Bridged Fe-Ni Heterointerfaces Confined in Hierarchical Mo_xC/N-Doped Carbon Enable Bifunctional Pathway for Efficient Oxygen Evolution

Cheol Ju Kim[a+], Seungjoon Ha[b+], Yun Jae Lee[a], Yun Min Kim[c], Hyun Jin Kim[a], Haeseong Jang[a,c], Seunghwa Lee*[b], and Seung-Keun Park*[a,c]

[a] *Department of Intelligent Energy and Industry, Chung-Ang University, 84 Heukseok-ro, Dongjak-gu, Seoul 06974, Republic of Korea*

[b] *Department of Chemical Engineering, Changwon National University, Changwon, 51140, Republic of Korea*

[c] *Department of Advanced Materials Engineering, Chung-Ang University, 4726, Seodong-daero, Daedeok-myeon, Anseong-si, Gyeonggi-do 17546, Republic of Korea*

+These authors contributed equally to this work

*Corresponding author.

E-mail address: seunghwa@changwon.ac.kr (S. Lee) skpark09@cau.ac.kr (S. -K. Park)

Characterizations of Materials

Scanning electron microscopy (SEM, HITACHI S-5000) and field-emission transmission electron microscopy (FE-TEM, JEM-2100F, Korea Basic Institute (Daegu)) were used to determine the morphology and architecture of the fabricated specimens. Powder X-ray diffraction (XRD) utilizing Cu Kα radiation (λ = 1.54060 Å) was conducted to validate their crystallographic phases. The chemical compositions of the samples were analyzed using X-ray photoelectron spectroscopy (XPS). Elemental analysis was conducted using inductively coupled plasma-optical emission spectrometry (ICP-OES; Optima 4300 DV). XANES spectra and EXAFS spectra were measured using the BL10C beamline at the Pohang Light Source (PLS-II) in Korea.

Raman spectroscopy

The catalyst ink was prepared by dispersing 10 mg of the catalyst in a mixed solvent consisting of 450 μL of deionized water, 450 μL of isopropanol, and 100 μL of Nafion solution. The mixture was sonicated for 30 minutes to achieve a homogeneous ink. Afterward, 10 μL of the ink was drop-cast onto a gold (Au) foil, achieving a catalyst loading of approximately 0.2 mg cm-2. The coated electrode was then dried at 70 °C for 30 minutes.

Operando Raman spectroscopy was conducted using a three-electrode configuration, where the catalyst-deposited Au foil served as the working electrode, a platinum wire served as the counter electrode, and a double-junction Ag/AgCl (3 M KCl) electrode was used as the reference electrode. The electrolyte employed was a 1 M KOH aqueous solution. Operando Raman spectra were recorded at open-circuit potential (OCP) and at various applied potentials ranging from 1.2 V to 1.6 V versus the reversible hydrogen electrode (RHE) in 0.05 V increases. The experiments were performed using a handmade Teflon cell at room temperature. The Raman spectrometer was equipped with a 532 nm laser, a 60× water-immersion objective,

and an 1800 mm^{-1} grating. For each spectrum, 30 scans were collected with an acquisition time of 1 second per scan. To ensure the reliability of the spectra, peak calibration was conducted using standard acetaminophen peaks prior to the measurements.

Electrochemical measurement

The electrochemical measurements were performed using a three-electrode system equipped with a ZIVE-SP1 instrument (WonATech Corp., Korea). Nickel foam (NF, geometric area: 1 cm^2), Pt wire, and Hg/HgO were employed as the working, counter, and reference electrodes, respectively. To prepare the working electrode, catalysts (5 mg) were added into 225 μL of 2-propanol and 225 μL of DI-water containing 50 μL of 5 wt.% Nafion solution, followed by sonication for 15 min and subsequent stirring overnight. After that, 110 μL of the prepared suspension was quantitatively dropped onto the surface of NF. The loading content of the catalyst on the working electrode is ~1.1 mg cm^{-2}. Electrochemical impedance spectroscopy (EIS) was performed in the frequency range of 0.1 Hz to 100 kHz. The Nyquist plots are presented after solution resistance (Rs) compensation, where Rs was determined from the high-frequency intercept of the raw data. This approach allows for a more accurate and direct comparison of the intrinsic charge-transfer behavior (R_{ct}) among the catalysts. To convert the measured potential to RHE, the equation $E_{RHE} = E_{Hg/HgO} + 0.0591 \times pH + 0.098$ V was used. Turnover frequency (TOF) of the catalysts were calculated by normalizing them to the total metal content according to the following equation:

$$TOF\ [e/(site \cdot s)] = \frac{J}{n_{metal} \times F} = \frac{J \times M_{metal}}{m_{cat.} \times w_{metal} \times F} \qquad (1)$$

where J is the kinetic current density, $m_{cat.}$ is the mass loading of the catalyst on the nickel foam, w_{metal} is the mass concentration of the metal in the catalyst, n_{metal} is the molar amount of the metal in the catalyst, and M_{metal} is the atomic weight of the metal.

The mass activity and specific activity of the catalysts were calculated by normalizing them to the total metal content according to the following equation:

$$Mass\ activity\ (mA\ mg_{metal}{}^{-1}) = \frac{J}{m_{cat.} \times w_{metal}} \quad (2)$$

$$Specific\ activity\ (\mu A\ cm_{ECSA}{}^{-2}) = \frac{J}{ECSA} \quad (3)$$

ECSA was calculated from the C_{dl} using ECSA = C_{dl}/C_s, where C_s was assumed to be 40 μF cm^{-2} (in alkaline media)."

AEMWE test

The electrocatalysts were deposited onto pressed Ni foam substrates via a catalyst-coated substrate (CCS) method. The catalyst loading on the anode was approximately 20 mg cm^{-2}, while a commercial Pt/C (40 wt%, TANAKA) catalyst with a loading of 1 mg cm^{-2} on carbon cloth was employed as the cathode. Subsequently, the anion exchange membrane water electrolyzer (AEMWE) was assembled into a membrane electrode assembly (MEA) using a Piperion A20 membrane (20 μm thickness). The polarization curves were recorded at a scan rate of 1 mV s^{-1} under continuous 1.0 M KOH flow at a rate of 100 mL min^{-1}. The geometric surface areas of both anode and cathode were 4 cm^2. Durability was further evaluated by chronopotentiometry at a constant current density of 0.5 A cm^{-2}.

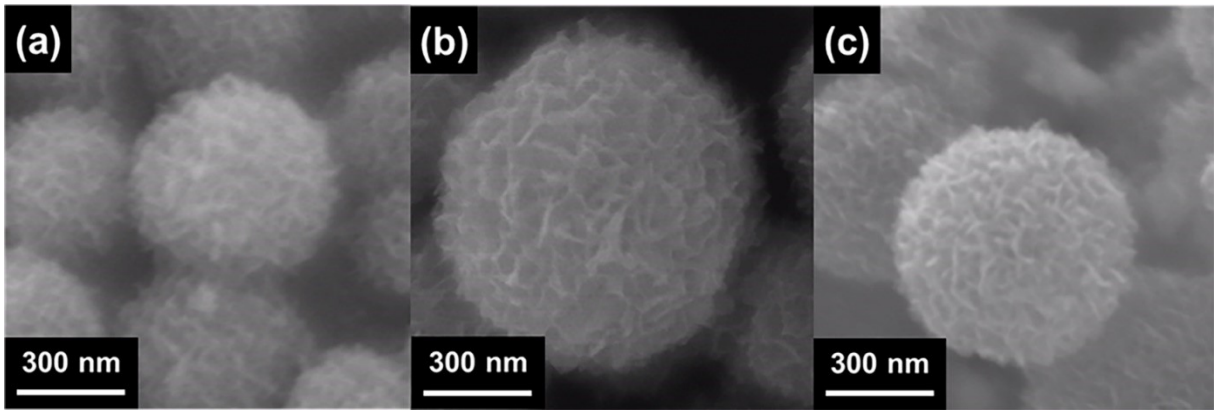

Fig. S1 SEM images of (a) Mo/PDA, (b) Ni-Mo/PDA, (c) NiO-Mo_xC/NC.

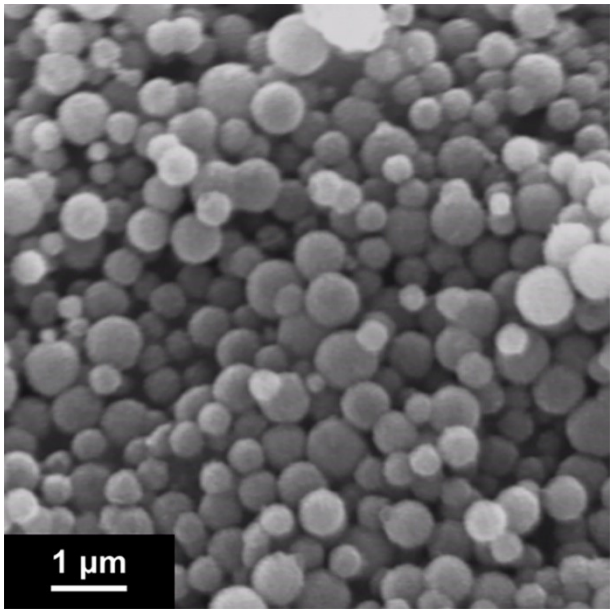

Fig. S2 Low-magnification SEM image of FeOOH-NiO@Mo_xC/NC.

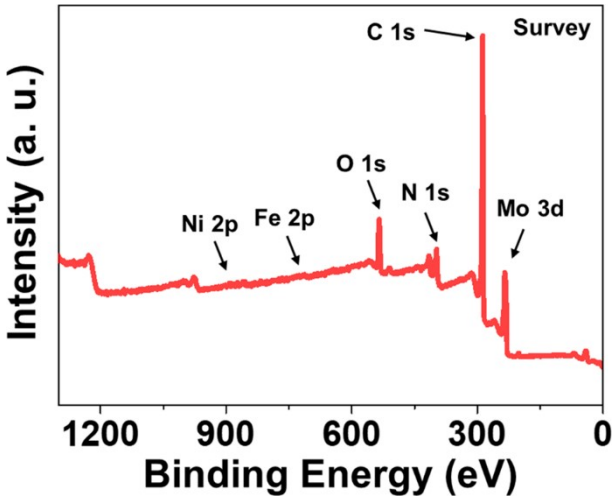

Fig. S3 Survey XPS spectra of FeOOH-NiO@Mo_xC/NC.

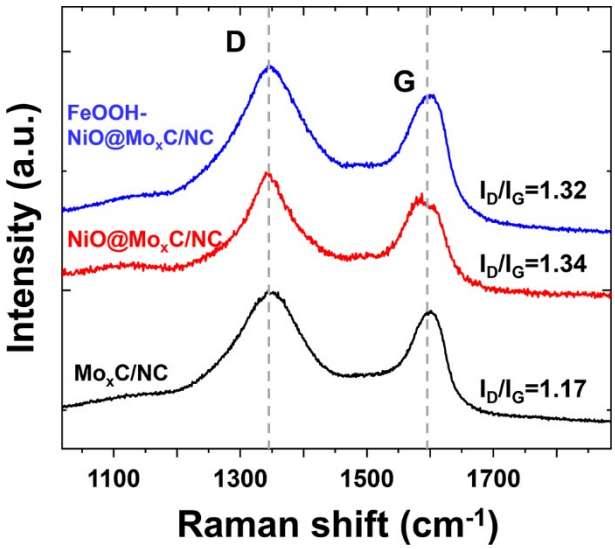

Fig. S4 Raman spectra of FeOOH-NiO@Mo_xC/NC, NiO@Mo_xC/NC, and Mo_xC/NC in the D- and G-band regions. The intensity ratio (I_D/I_G) serves as an indicator of structural disorder.

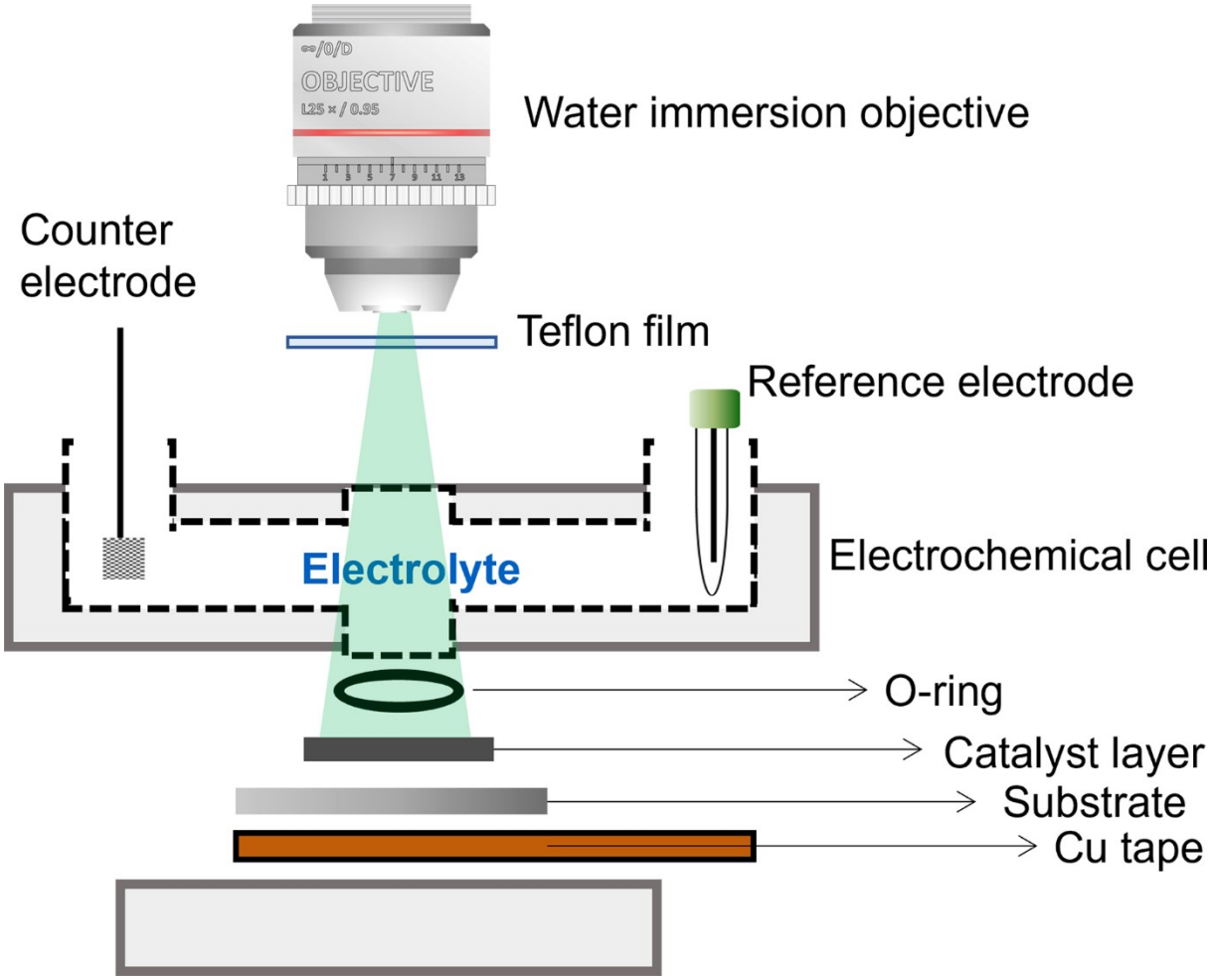

Fig. S5 Schematic illustration of the operando Raman spectroscopic setup used for electrochemical measurements.

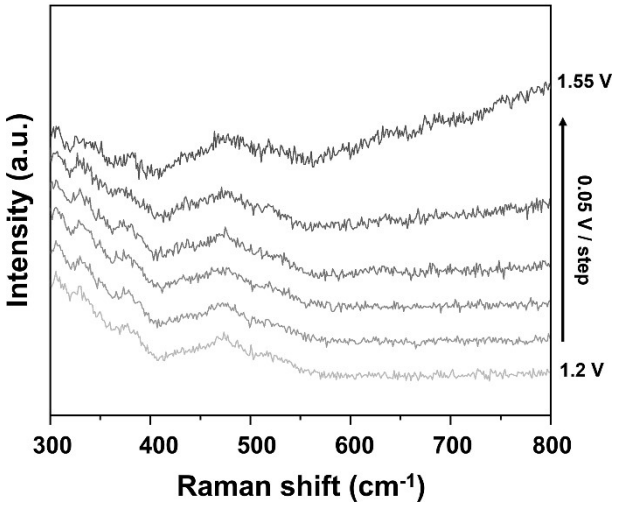

Fig. S6 Potential-dependent operando Raman spectra of Mo_xC/NC obtained in the potential range of 1.20–1.45 V (vs. RHE) with 0.05 V step intervals.

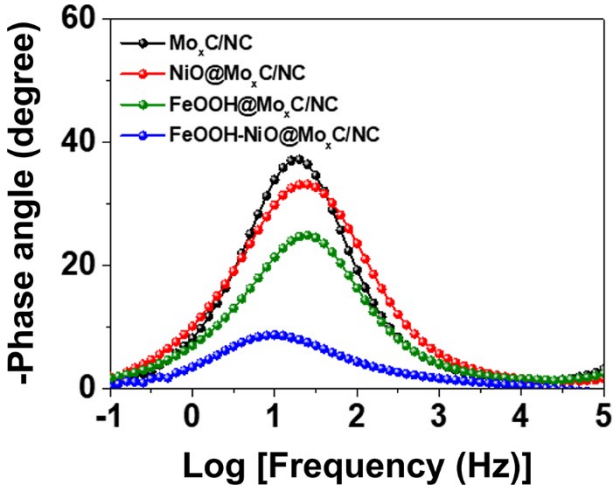

Fig. S7 The Bode plots obtained at 1.60 V (vs. RHE).

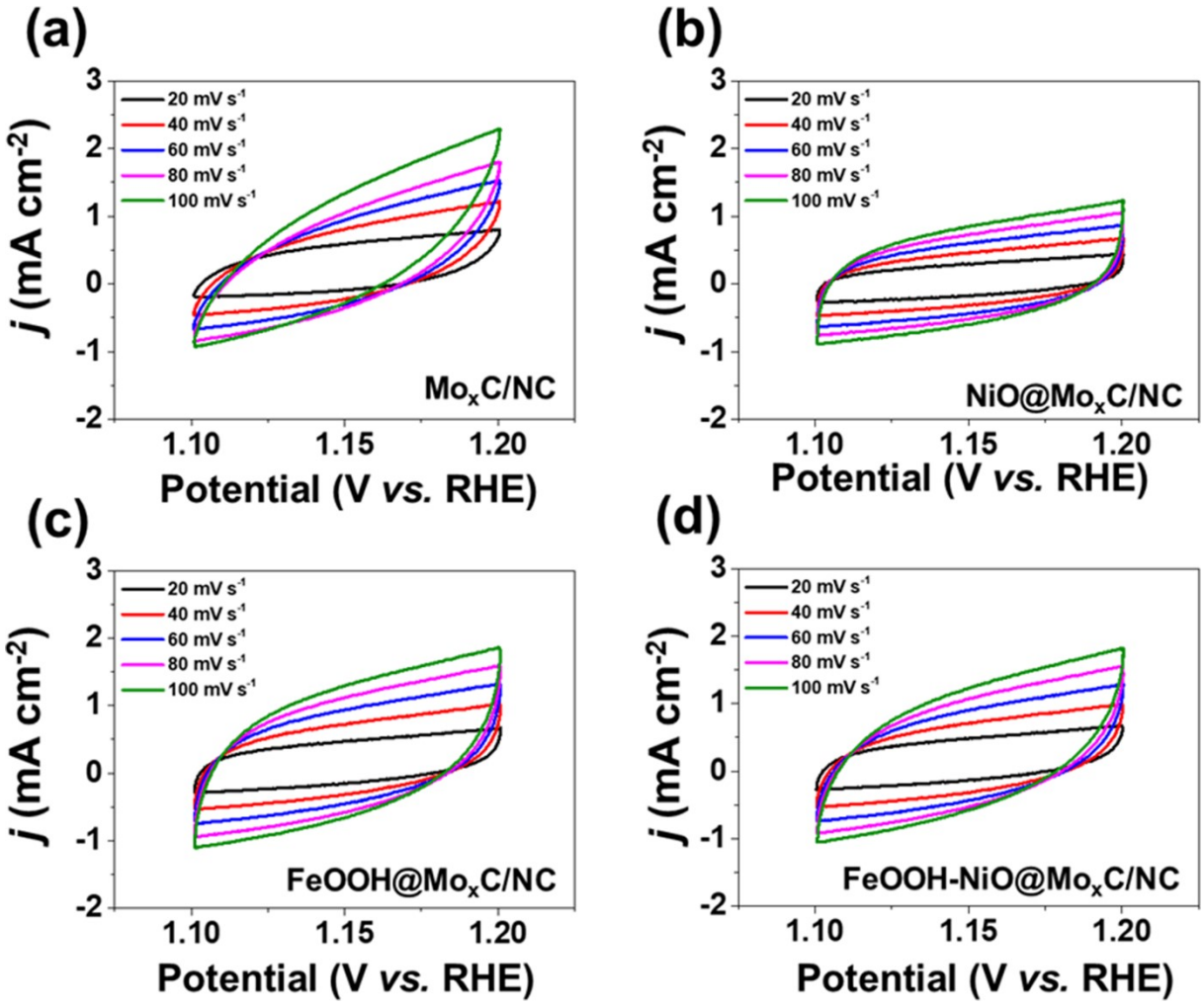

Fig. S8 (a-d) Cyclic voltammetry curves of different samples at different scan rates under potential from 1.1 to 1.2 V (vs. RHE).

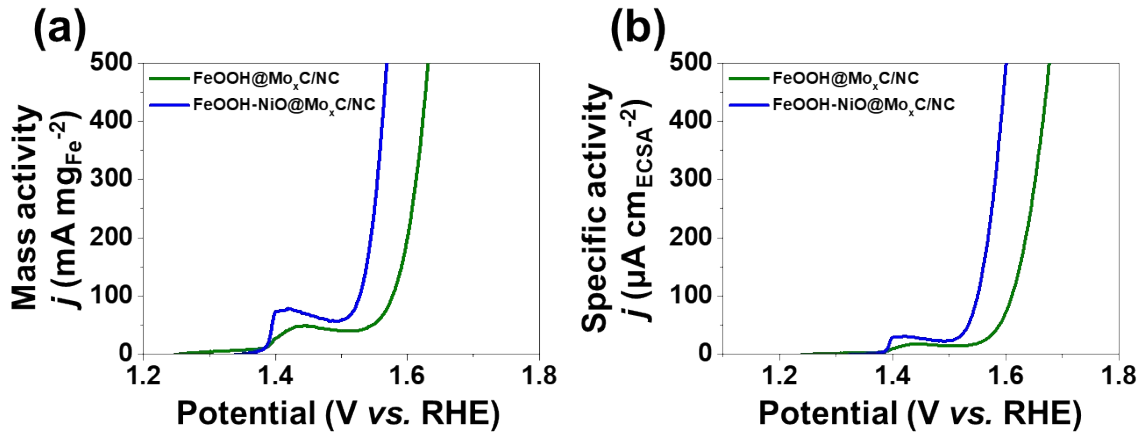

Fig. S9. (a) LSV curves for OER showing mass activity normalized to the Fe content based on ICP-OES analysis in 1 M KOH. (b) LSV curves for OER showing specific activity normalized to the ECSA.

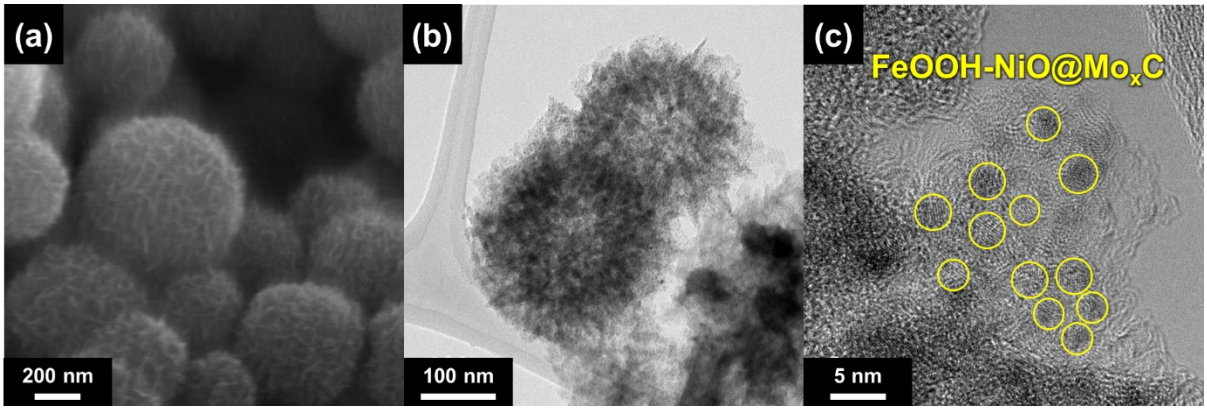

Fig. S10. (a) SEM image and (b, c) HRTEM images of FeOOH-NiO@Mo_xC/NC after ADT.

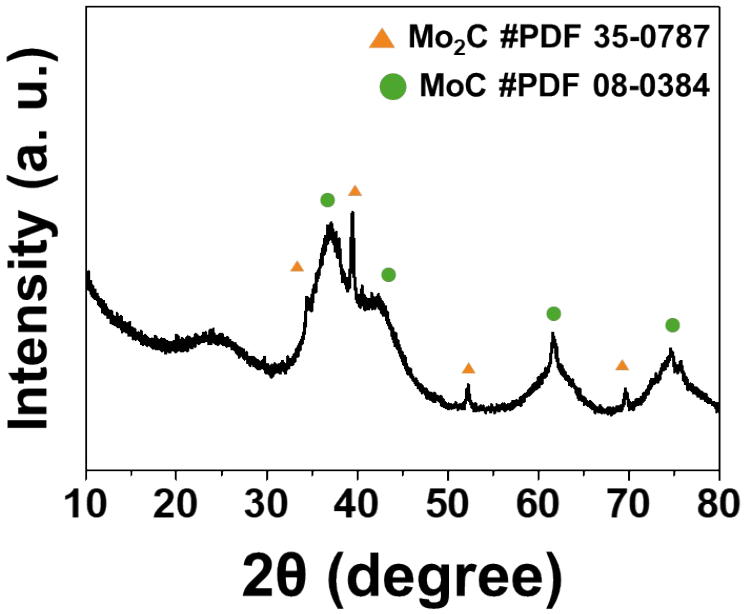

Fig. S11. XRD patterns of FeOOH-NiO@Mo_xC/NC after ADT.

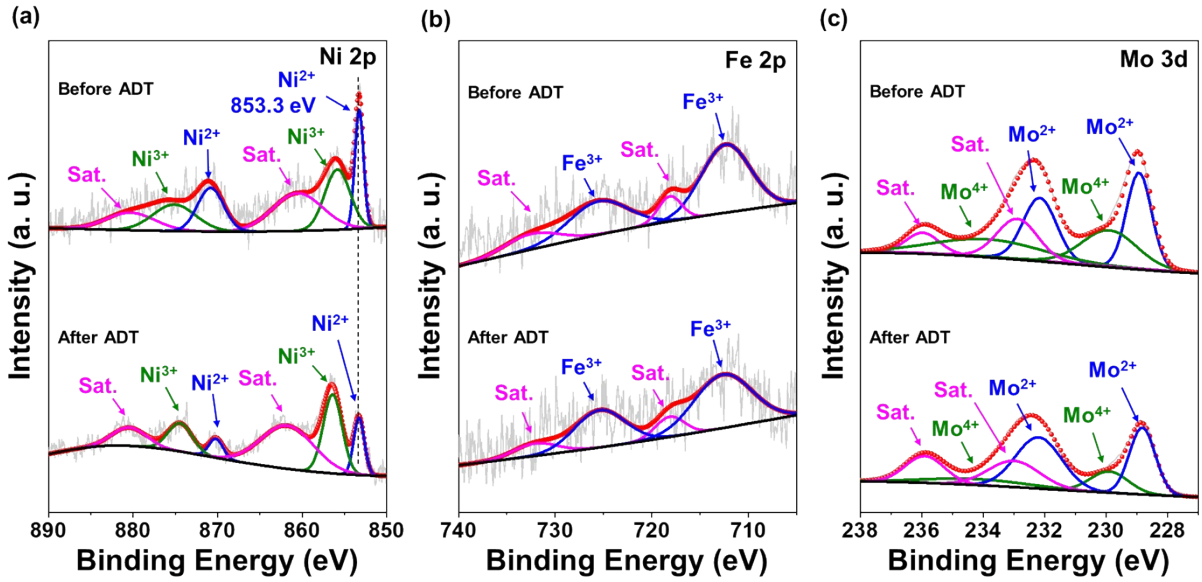

Fig. S12. Comparison of XPS spectra of (a) Fe 2p, (b) Ni 2p, and (c) Mo 3d for FeOOH-NiO@Mo_xC/NC before and after ADT.

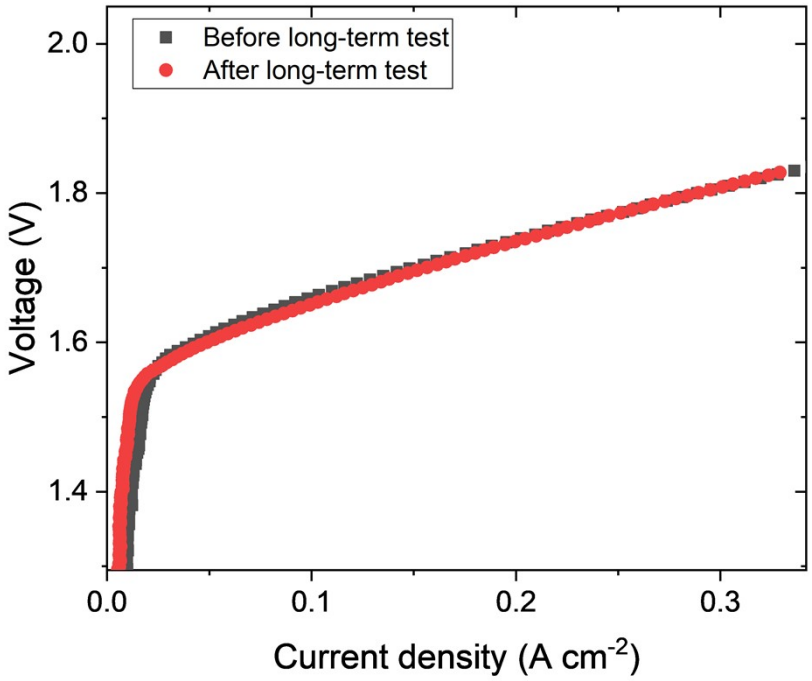

Fig. S13. Single-cell polarization curves of the AEMWE employing FeOOH-NiO@Mo_xC/NC as the anode, recorded before and after the 300 h durability test at 500 mA cm^{-2}.

Table S1. ICP-OES result of FeOOH-NiO@Mo_xC/NC.

Sample	Element	Concentration (mg/kg)	Molar ratio
FeOOH-NiO@Mo_xC/NC	Mo	479,000	1
	Ni	25,000	0.085
	Fe	6,800	0.024

Table S2. O 1s XPS spectra of FeOOH-NiO@Mo_xC/NC, NiO@Mo_xC/NC, and Mo_xC/NC. The table shows the deconvoluted peak area ratios corresponding to M-OH, M-O, and adsorbed H_2O species.

	M-OH ratio (%)	**M-O ratio (%)**	**Absorbed H_2O ratio (%)**	**Total** (%)
FeOOH-NiO@Mo_xC/NC	31.7	32.9	35.4	100
NiO@Mo_xC/NC	12.3	56.5	31.1	100
Mo_xC/NC	6.2	34.1	59.7	100

Table S3. Electrochemical performance comparison of the reported catalysts, including overpotential at a current density of 100 mA cm^{-2}, Tafel slope, and stability.

Catalysts	Electrolyte	Overpotential at 100 mA cm^{-2} (mV)	Tafel slope (mV dec^{-1})	Stability	Ref.
FeOOH-NiO @Mo_xC/NC	**1 M KOH**	**372**	**77.8**	**80 h at 100 mA cm^{-2}**	**This work**
$FeNi_3N$-NPs	1 M KOH	386	42	9 h at 10 mA cm^{-2}	[S1]
NF/Co_3O_4-Ni	1 M KOH	390	59.5	12 h at 70 mA cm^{-2}	[S2]
Ni/Fe_3O_4	1 M KOH	393	70	11 h	[S3]
FeNi-LDH Ss/Ni	1 M KOH	409	85.7	12 h at 1.52 V (*vs.* RHE)	[S4]
P-$Ni_{0.5}Fe_{0.5}Se_2$	1 M KOH	428	73	12 h at 10 mA cm^{-2}	[S5]
RuO2	1 M KOH	436	120.1	-	This work

Reference

1 X. Jia, Y. Zhao, G. Chen, L. Shang, R. Shi, X. Kang, G. I. N. Waterhouse, L.Z. Wu, C.H. Tung and T. Zhang, *Advanced Energy Materials*, 2016, **6**, 1502585.

2. L. Zeng, K. Zhou, L. Yang, G. Du, L. Liu and W. Zhou, *ACS Applied Energy Materials*, 2018, **1**, 6279-6287.

3. C. He, X. Kong, M. Jiang and X. Lei, *Materials Letters*, 2018, **222**, 138-141.

4. P. Xu, J. Li, J. Luo, L. Wei, D. Zhang, D. Zhou, W. Xu and D. Yuan, *Sci. Rep.*, 2018, **8**, 9425.

5. L. Lv, Z. Li, Y. Ruan, Y. Chang, X. Ao, J.-G. Li, Z. Yang and C. Wang, *Electrochim. Acta*, 2018, **286**, 172-178.

6. K. Fan, H. Chen, Y. Ji, H. Huang, P. M. Claesson, Q. Daniel, B. Philippe, H. Rensmo, F. Li, Y. Luo and L. Sun, *Nat. Commun.*, 2016, **7**, 11981.

7. F. Dionigi, J. Zhu, Z. Zeng, T. Merzdorf, H. Sarodnik, M. Gliech, L. Pan, W.-X. Li, J. Greeley and P. Strasser, *Angew. Chem.*, 2021, **60**, 14446-14457.

8. L. Ciambriello, I. Alessandri, L. Gavioli and I. Vassalini, *ChemCatChem*, 2024, **16**, e202400286.

9. A.-L. Wang, Y.-T. Dong, M. Li, C. Liang and G.-R. Li, *ACS Applied Materials & Interfaces*, 2017, **9**, 34954-34960.

10. X. Yu, M. Zhang, Y. Tong, C. Li and G. Shi, *Advanced Energy Materials*, 2018, **8**, 1800403.

11. S. Zhao, M. Li, M. Han, D. Xu, J. Yang, Y. Lin, N.-E. Shi, Y. Lu, R. Yang, B. Liu, Z. Dai and J. Bao, *Adv. Funct. Mater.*, 2018, **28**, 1706018.